SEMARAK ILMU PUBLISHING

Journal of Advanced Research in Fluid Mechanics and Thermal Sciences

Journal homepage: https://semarakilmu.com.my/journals/index.php/fluid_mechanics_thermal_sciences/index
ISSN: 2811-3950

Stagnation Point Flow of a Hybrid Nanofluid Under the Gravity Modulation Effect

Mohamad Hidayad Ahmad Kamal[1], Anati Ali[1], Lim Yeou Jiann[1], Noraihan Afiqah Rawi[1,*], Sharidan Shafie[1]

[1] Department of Mathematical Sciences, Faculty of Science, Universiti Teknologi Malaysia, 81310 UTM, Johor Bahru, Johor Darul Takzim, Malaysia

ARTICLE INFO

Article history:
Received 17 July 2021
Received in revised form 28 December 2022
Accepted 8 January 2022
Available online 23 February 2022

ABSTRACT

The effectiveness of the heat transfer fluid in the cooling or heating process determines the optimal performance of the nuclear reactor, microelectronic devices, and chip production. Since thermal conductivity improved in hybrid nanofluids, the current study sought to investigate the unsteady free convection hybrid nanofluid flow near a stagnation point as influenced by g-jitter. A hybrid nanofluid consisted of copper (Cu) and alumina (Al_2O_3) nanoparticles, which were added into water to form Cu-Al_2O_3/water was considered. Next, relevant variables transformed the governing equation into dimensionless equations before being solved numerically using a centered implicit finite difference method. The fluid field and heat transfer were discussed concerning the stagnation point curvature ratio. The results showed that the g-jitter effect caused fluctuation in all profiles and physical quantities. The frequency and amplitude of the g-jitter reduced the velocity profile while improving the temperature distribution. The heat transfer rate increased by 10.77% when the hybrid nanoparticles volume fractions rose from 0.1 to 0.2. However, the presence of hybrid nanoparticles had reduced the thickness of the momentum boundary layer due to an increase in the local skin friction.

Keywords:
hybrid nanofluid; stagnation point flow; g-jitter

1. Introduction

The flow problem in heat transfer has recently received much attention, either experimentally or theoretically. Water, oil, and ethylene glycol are conventional heat transferring fluids with poor thermal physical properties. Due to technological advancements, a better cooling system was designed to meet demand. In 1995, Choi and Eastman [1] added a small number of copper nanoparticles to a conventional fluid. They found out that the fluid's conductivity had improved. Studies on boundary layer flow also had a significant impact on this discovery, where several mathematical models were introduced to describe the properties of nanofluids. Based on their study, the Brownian motion and thermophorosis effect were factored in the Buongiorno nanofluid model [2]. The Tiwari and Das nanofluid model, on the other hand, was focused on the effect of the types

* *Corresponding author.*
E-mail address: noraihanafiqah@utm.my

https://doi.org/10.37934/arfmts.92.2.157170

and volume fraction of the nanoparticles used [3]. Many theoretical studies on Newtonian nanofluid boundary layer flow have been conducted, considering various factors [4–8]. Other exciting studies were also conducted using multiple nanoparticles to evaluate their performance on heat transfer enhancement [9–12].

Subsequently, a nanofluid known as 'hybrid nanofluid' was designed to improve the thermophysical properties of regular nanofluid. Due to synergistic effects, hybrid nanofluid contains two or more nanoparticles with new thermophysical and chemical properties, enhancing the heat transfer rate. Several experimental studies in hybrid nanofluid flow were carried out, with the researchers introducing some new correlations [13–16]. Among these, some have demonstrated that using a hybrid nanofluid could result in a better fluid system in heat transfer advancement [17, 18] Moghadassi *et al.,* [17] investigated the flow and convective heat transfer properties of water-based Al_2O_3 and $Cu–Al_2O_3$ hybrid nanofluids with 0.1% volume concentration. When compared to the classical nanofluid, the hybrid had a higher convective heat transfer coefficient.

On the other hand, Kashyap and Dass [19] performed a theoretical analysis on hybrid nanofluids with three different boundary conditions. The higher heat transfer rate was observed at a lower Richardson number because of the significant aiding effect of shear force on the buoyancy force. Wahid *et al.,* [20] recently investigated the effect of a shrinking sheet with suction and thermal radiation on a hybrid nanofluid. Their finding showed that the presence of the hybrid nanoparticle could reduce boundary layer separation. Meanwhile, Khashi'ie *et al.,* [21] investigated the unsteady hybrid $Cu\text{-}Al_2O_3$/water nanofluid over a stretched/shrunk disc with convective boundary conditions.

Stagnation point flow has substantial properties in the fluid flow where the highest local pressure is located [22]. Three-dimensional cases were used to conduct theoretical research on stagnation point nanofluid flow [23–25]. Sulochana and Sandeep [26] studied the Cu-water nanofluid's stagnation point flow and heat transfer behavior against a horizontal and exponentially permeable stretching/shrinking cylindrical body. On the other hand, Rehman *et al.,* [25], conducted a theoretical investigation into a water-based nanofluid three-dimensional magnetohydrodynamic (MHD) stagnation-point flow with heat and mass transport over an exponentially stretched surface. The unsteady MHD $Al_2O_3\text{-}Cu/H_2O$ hybrid nanofluid near a stagnation point with heat source/sink influence was also investigated by Zainal *et al.,* [28]. Consequently, the advancement of nanofluid on stagnation point flow was broadened by inducing hybrid nanofluid, with most of the study was conducted either for Newtonian and non-Newtonian types of fluid [29–32].

Nadeem *et al.,* [29] investigated a three-dimensional stagnation point flow of a hybrid nanofluid past a circular cylinder with and without thermal slip effects. As per findings, a positive value of the thermal slip parameter was inversely proportional to the temperature profile of either the nanofluid or the hybrid nanofluid. Khashiie *et al.,* [31] examined the flow and heat transfer of a non-axisymmetric hybrid $Cu\text{-}Al_2O_3$/water nanofluid over a stretching/shrinking flat plate near a Homann stagnation point. They concluded that an increase in the ambient fluid strain rate ratio to the plate strain rate would prolong and hasten the separation of the boundary layer from the sample.

Gravitational force is one of the forces that affect transportation matter as part of the body forces. Outer space is assumed as an area where gravity forces do not affect the phenomena. Interestingly, a fluctuating microgravity effect, a nonsexist effect on Earth, was discovered during the experiment on outer space. The fluctuating gravitational field is later referred to as the g-jitter effect, and it is discovered to have a significant impact on the experimental results obtained in outer space [20]. Hamdan *et al.,* [33], investigated the influence of the g-jitter and heat generation on a three-dimensional free convection stagnation point of a boundary layer flow. They also analyzed the effect of the geometry of the stagnation point on flow behavior. Other researchers also reported the impact of g-jitter on boundary layer nanofluid flow in determining different types of nanoparticles and other nanoparticle properties [34–37].

Meanwhile, Rawi *et al.,* [38] analyzed an uncontrolled mixed convection flow of second-grade fluid over an inclined stretching plate influenced by nanoparticles of various shapes, using carboxymethyl cellulose as the base fluid. The g-jitter effect on the stagnation point of a boundary layer flow was numerically or analytically studied [39–41]. Subsequently, a nanofluid was also implemented to evaluate its effect on the g-jitter [42, 43]. Their study observed that the thermal properties of the fluid system were enhanced when the gravitational field fluctuated.

Theoretical studies combining the hybrid nanofluid, stagnation point, and g-jitter effects are scarce. Based on the above-discussed literature, research on nanofluid, hybrid nanofluid, stagnation point, and g-jitter effects have been combined separately or partially with the boundary layer flow with various fluid system configurations and boundary conditions. Thus, a numerical study of a hybrid nanofluid flow induced by gravity modulation near a three-dimensional stagnation point was conducted. Cu and Al_2O_3 composite hybrid nanoparticles were used to characterize a water-based hybrid nanofluid. The mathematical modeling of a fluid system subjected to no-slip boundary conditions was solved using the Maple solver "pdsolve," which implemented the implicit centered finite difference method. Existing hybrid nanoparticles and g-jitter on fluid behavior and thermal properties were graphically depicted and discussed.

2. Mathematical Formulation

The flow of a free convection hybrid nanofluid induced by a g-jitter near a three-dimensional stagnation point was studied. The water-based hybrid nanofluid was assumed to be an incompressible, unsteady viscous fluid. In this study, Cu and Al_2O_3 were chosen as nanoparticles, and the experiment was conducted under a no-slip boundary condition. The body's surface had a constant temperature, T_w, while T_∞ denotes the ambient fluid's temperature in the free stream. At the body's surface, there is a point where its located the local velocity equals zero, where high pressure existed at the point. It is known as the stagnation point, particularly the nodal point, N. In this study, N was chosen to represent the stagnation point flow, which was then denoted in a Cartesian orthogonal system (x, y, z), where N was located at the origin (Figure 1). The stagnation point flow characteristics were defined in terms of parameters a and b (see Eq. (2) and (3)), whereby $|a| \geq |b|$, with $a > 0$ and $c = b/a$. The stagnation point is at a cylinder and spherical surface if $c = 0$ and $c = 1$, respectively. The $x-$ and $y-$coordinates were measured parallel to the body surface, while the $z-$coordinate was measured normal.

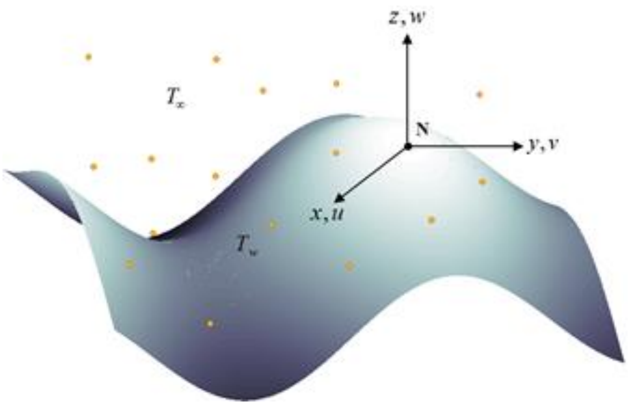

Fig. 1. Physical model representation in the Cartesian coordinate system

When the g-jitter effect was considered, the gravitational field is mathematically defined as:

$$g(t) = g_0\left[1+\varepsilon\cos\left(\pi\omega t\right)\right] \tag{1}$$

where g_0 is the gravitational acceleration mean, ε is the scaling parameter representing the amplitude of the gravity modulation, ω is the frequency of oscillation for the flow induced by the g-jitter, and t is the dimensional time parameter. The mathematical model was then simplified by using Prandtl's assumption [44]. Therefore, the equation system for the unsteady hybrid nanofluid boundary layer flow at three-dimensional stagnation point with g-jitter effect after boundary layer and Boussinesq approximation is as follows [43, 45]:

$$\rho_{nf}\left(\frac{\partial u}{\partial t}+u\frac{\partial u}{\partial x}+v\frac{\partial u}{\partial y}+w\frac{\partial u}{\partial z}\right)=\mu_{hnf}\frac{\partial^2 u}{\partial z^2}+g(t)\left(\rho\beta\right)_{hnf}ax\left(T-T_\infty\right), \tag{2}$$

$$\rho_{nf}\left(\frac{\partial v}{\partial t}+u\frac{\partial v}{\partial x}+v\frac{\partial v}{\partial y}+w\frac{\partial v}{\partial z}\right)=\mu_{hnf}\frac{\partial^2 v}{\partial z^2}+g(t)\left(\rho\beta\right)_{hnf}by\left(T-T_\infty\right), \tag{3}$$

$$\frac{\partial T}{\partial t}+u\frac{\partial T}{\partial x}+v\frac{\partial T}{\partial y}+w\frac{\partial T}{\partial z}=\alpha_{hnf}\frac{\partial^2 T}{\partial z^2}, \tag{4}$$

subject to

$$\begin{aligned}
&t=0: u=v=w=0, T=T_\infty \text{ for any } x, y \text{ and } z,\\
&t>0: u=v=w=0, T=T_w \text{ on } z=0, x\ge 0, y\ge 0,\\
&\qquad u=v=0, \qquad T=T_\infty \text{ on } x=0, y\ge 0, z\ge 0,\\
&\qquad u=v=0, \qquad T=T_\infty \text{ on } y=0, x\ge 0, y\ge 0,\\
&\qquad u=v=0, \qquad T=T_\infty \text{ as } z\to\infty, x\ge 0, y\ge 0.
\end{aligned} \tag{5}$$

The velocity component along the direction x, y, and z axes is represented by u, v, and w respectively, and T is the hybrid nanofluid's dimensional temperature parameter. The thermophysical properties of the hybrid nanofluid were carried out by subscribing with the term hnf. Notation ρ, μ, β, and α denote the density, dynamic viscosity, thermal expansion, and thermal diffusion, respectively. As suggested by [46], we employed the equations to evaluate the thermophysical properties of the hybrid nanofluid as given:

$$\mu_{nf} = \frac{\mu_f}{\left[1-\left(\phi_{Cu}+\phi_{Al_2O_3}\right)\right]^{2.5}}, \alpha_{hnf} = \frac{k_{hnf}}{\left(\rho c_p\right)_{hnf}},$$
$$\rho_{hnf} = \left(1-\phi_{hnf}\right)\rho_f + \phi_{Cu}\rho_{Cu} + \phi_{Al_2O_3}\rho_{Al_2O_3},$$
$$\left(\rho\beta\right)_{hnf} = \left(1-\phi_{hnf}\right)\left(\rho\beta\right)_f + \phi_{Cu}\left(\rho\beta\right)_{Cu} + \phi_{Al_2O_3}\left(\rho\beta\right)_{Al_2O_3},$$
$$\left(\rho c_p\right)_{hnf} = \left(1-\phi_{hnf}\right)\left(\rho c_p\right)_f + \phi_{Cu}\left(\rho c_p\right)_{Cu} + \phi_{Al_2O_3}\left(\rho c_p\right)_{Al_2O_3}, \tag{6}$$
$$\frac{k_{hnf}}{k_f} = \frac{\dfrac{\phi_{Cu}k_{Cu}+\phi_{Al_2O_3}k_{Al_2O_3}}{\phi_{hnf}} + 2k_f + 2\left(\phi_{Cu}k_{Cu}+\phi_{Al_2O_3}k_{Al_2O_3}\right) - 2k_f\phi_{hnf}}{\dfrac{\phi_{Cu}k_{Cu}+\phi_{Al_2O_3}k_{Al_2O_3}}{\phi_{hnf}} + 2k_f - \left(\phi_{Cu}k_{Cu}+\phi_{Al_2O_3}k_{Al_2O_3}\right) - 2k_f\phi_{hnf}}$$

Here, ϕ is defined as the nanoparticle volume fraction, which is the nanoparticle concentration that is added into the fluid. k and c_p are defined as the thermal conductivity and specific heat capacity, respectively. The subscript *Cu*, *Al_2O_3*, and f represent the copper, alumina, and fluid components in the hybrid nanofluid mixture. The thermophysical properties are shown in Table 1 [45, 46].

Table 1
Thermophysical properties at a temperature of 20 °C in the atmosphere

Physical Properties	Al_2O_3	Cu	Water
Density ρ, (kgm^{-3})	3970	8933	997.1
Specific heat capacity c_p, $(\mathrm{Jkg}^{-1}K^{-1})$	765	385	4179
Thermal conductivity k, $(\mathrm{Wm}^{-1}K^{-1})$	40	400	0.613
Thermal expansion $\beta \times 10^{-5}$, (K^{-1})	0.85	1.67	21

The semi-similar transformation technique was then used to reduce the problem's complexity. The variables are as follows [40]:

$$\eta = Gr^{1/4}az, \quad \tau = \Omega t, \quad t = \upsilon a^2 Gr^{1/2} t^*,$$
$$u = \upsilon a^2 x Gr^{1/2} f', \quad v = \upsilon a^2 y Gr^{1/2} h', \quad w = -\upsilon a Gr^{1/4}\left(f+h\right), \tag{7}$$
$$\Omega = \frac{\omega}{\upsilon a^2 Gr^{1/2}}, \quad \theta = \frac{\left(T-T_\infty\right)}{\left(T_w-T_\infty\right)}, \quad Gr = \frac{g_0\beta\left(T-T_\infty\right)}{a^3\upsilon^2},$$

where υ is the fluid's kinematic viscosity, and Gr is the thermal Grashof number. The prime notation at the top of the function f and h indicate the differentiation concerning η. Here, θ and Ω are dimensionless variables for temperature and oscillation frequency, respectively. Using semi-similar variables in (7), the $x-$direction momentum, $y-$direction momentum, and energy in Eq. (2), (3), and (4), respectively, were transformed into dimensionless governing equations that depending on two dependent variables, such that,

$$C_1 f''' + C_2(f+h)f'' - C_2 f'^2 + C_3\left[1+\varepsilon\cos\left(\pi\tau\right)\right]\theta = C_2\Omega\frac{\partial f'}{\partial\tau}, \tag{8}$$

$$C_1 h''' + C_2 (f+h) h'' - C_2 h'^2 + cC_3 \left[1+\varepsilon \cos\left(\pi\tau\right)\right]\theta = C_2 \Omega \frac{\partial h'}{\partial \tau}, \tag{9}$$

$$\frac{C_4}{C_5 \Pr}\theta'' + \left(f+h\right)\theta' = \Omega \frac{\partial \theta}{\partial \tau}, \tag{10}$$

whereby Pr is the Prandtl number, and the hybrid nanofluid properties are given by:

$$\begin{gathered}
C_1 = \frac{1}{\left(1-\phi_{Cu}-\phi_{Al_2O_3}\right)^{2.5}}, \quad C_2 = 1-\phi_{hnf} + \frac{\phi\rho_{Cu}}{\rho_f} + \frac{\phi\rho_{Al_2O_3}}{\rho_f}, \\
C_3 = 1-\phi_{hnf} + \frac{\phi\left(\rho\beta\right)_{Cu}}{\left(\rho\beta\right)_f} + \frac{\phi\left(\rho\beta\right)_{Al_2O_3}}{\left(\rho\beta\right)_f}, \quad C_5 = 1-\phi_{hnf} + \frac{\phi\left(\rho c_p\right)_{Cu}}{\left(\rho c_p\right)_f} + \frac{\phi\left(\rho c_p\right)_{Al_2O_3}}{\left(\rho c_p\right)_f}, \\
C_4 = \frac{\dfrac{\phi_{Cu}k_{Cu}+\phi_{Al_2O_3}k_{Al_2O_3}}{\phi_{hnf}} + 2k_f + 2\left(\phi_{Cu}k_{Cu}+\phi_{Al_2O_3}k_{Al_2O_3}\right) - 2k_f\phi_{hnf}}{\dfrac{\phi_{Cu}k_{Cu}+\phi_{Al_2O_3}k_{Al_2O_3}}{\phi_{hnf}} + 2k_f - \left(\phi_{Cu}k_{Cu}+\phi_{Al_2O_3}k_{Al_2O_3}\right) - k_f\phi_{hnf}}.
\end{gathered} \tag{11}$$

subjected to the dimensionless boundary condition

$$\begin{gathered}
f\left(\eta,0\right) = f\left(0,\tau\right) = f'\left(0,\tau\right) = 0, \quad h\left(\eta,0\right) = h\left(0,\tau\right) = h'\left(0,\tau\right) = 0, \\
\theta\left(\eta,0\right) = 0, \quad \theta\left(0,\tau\right) = 1, \\
f' \to 0, \quad h' \to 0, \quad \theta \to 0, \quad \text{as } \eta \to \infty.
\end{gathered} \tag{12}$$

The skin friction, C_f, and Nusselt number, Nu, were the primary physical quantities of interest in this study. Both physical quantities can be mathematically defined as follows:

$$\begin{aligned}
C_{fx} &= \mu_{nf}\left(\frac{\partial u}{\partial z}\right)_{z=0} \Big/ \left(\rho_f \upsilon^2 a^3 x\right), \\
C_{fy} &= \mu_{nf}\left(\frac{\partial v}{\partial z}\right)_{z=0} \Big/ \left(\rho_f \upsilon^2 a^3 y\right), \\
Nu &= -a^{-1}k_{nf}\left(\frac{\partial T}{\partial z}\right)_{z=0} \Big/ k_f\left(T_w - T_\infty\right).
\end{aligned} \tag{13}$$

The physical quantities were subjected to the same dimensionless procedure,

$$\begin{aligned}
C_{fx}/Gr^{3/4} &= f''\left(\tau,0\right)/\left(1-\phi_{hnf}\right)^{2.5}, \\
C_{fy}/Gr^{3/4} &= h''\left(\tau,0\right)/\left(1-\phi_{hnf}\right)^{2.5}, \\
Nu/Gr^{1/4} &= -\left(k_{hnf}/k_f\right)\theta'\left(\tau,0\right).
\end{aligned} \tag{14}$$

The governing Eq. (8)-(10) subjected to conditions (12) were solved using the Maple solver "pdsolve," which employs the finite difference method's centered implicit scheme. Dimensionless independent variables are denoted as follows:

$$\begin{aligned} &\tau^0 = 0, \quad \tau^n = \tau^{n-1} + k_n, \quad n = 1,2,\ldots,N, \\ &\eta_0 = 0, \quad \eta_j = \eta_{j-1} + h_j, \quad j = 1,1,\ldots,J, \end{aligned} \tag{15}$$

where is the spacing and is the spacing. The sequence numbers and indicate the coordinate location. The differential equations were then discretized using the centered different formula, implemented by the "pdsolve" solver. The Maple code for computing the numerical result is illustrated in Appendix A.

$$f'(\eta_j,\tau_n) \equiv \frac{1}{2h_j}\left(f_{j+1} - f_{j-1}\right), \quad \frac{\partial f(\eta_j,\tau_n)}{\partial \tau} \equiv \frac{1}{2k_n}\left(f^{n+1} - f^{n-1}\right), \tag{16}$$

3. Results and Discussion

The dimensionless system of equations in (7) – (9), as well as with the no-slip boundary conditions (11), was solved numerically. Based on the results of this analysis, this section critically discusses the fluid behavior characteristic and heat transfer properties via profiles and physical quantities. The effect of parameters, such as c, ε, Ω, and ϕ on the temperature and velocity distributions were analyzed and graphically presented. In terms of computation, the grid is set to be uniform for both η and τ, where $\Delta\eta = 0.04$ and $\Delta\tau = 0.1$, respectively. The solution was then converged when the absolute maximum difference between iterations was attained. For the following analysis, the influence of the pertinent parameters was taken in these ranges: $0 < c < 1$, $0 < \Omega < 1$, $0 < \varepsilon < 1$, and $0.1 < \phi_{hnf} < 0.2$ for $0 < \eta < 10$ and $0 < \tau < 3$.

Throughout the study, the effects were analyzed in terms of profiles and physical quantities. The velocity and temperature profiles in Figure 3 – 5 demonstrated natural convection. The velocity profile began at zero at the wall and increased as η increased, but it approached zero as it went to the free stream. As for the temperature profile, the behavior exhibited natural convection as the temperature approached zero as it went to the free stream. Figure 2 shows velocity profiles for various values of the curvature ratio, c , where c represents the geometrical shape of the boundary body at the nodal point of attachment. From the figure, there were no changes in the velocity profile in the $y-$direction at $c = 0$. This type of flow is known as plane stagnation point, and it occurs at a cylindrical body. At $c = 1$, the amplitude for velocity profile in the $x-$ and $y-$ direction is found to be the same. The curvature ratio of $c = 1$ represents a spherical body shape, and the flow case is known as an axisymmetric type of stagnation point flow.

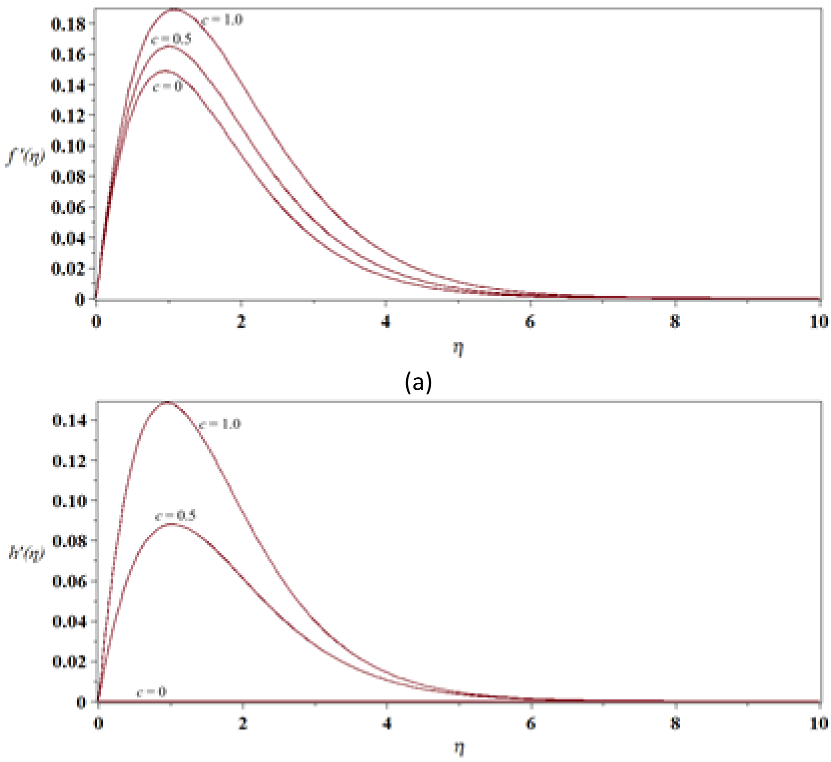

(a)

(b)

Fig. 2. The velocity profiles in (a) $x-$ and (b) $y-$direction due to various values of the geometry ratio c at the stagnation point

Figure 3 and 4 analyzed the g-jitter effect on the velocity and temperature profiles as represented by ε and Ω. When ε is increased, the velocity profile fluctuates in both directions while the temperature profile decreases. The fluctuation behavior is caused by the g-jitter properties, which generate a modulated type of gravitational field. On the other hand, Ω size reduced with the velocity curve in both directions and the temperature profile. Furthermore, as the Ω parameters increased, the boundary layer thickness for both the velocity profiles decreased. As ε improved, the fluctuation behavior was also observed in physical quantities, as shown in Table 2. The fluctuation behavior was caused by the presence of the g-jitter effect on the fluid system. It is also worth noting that the most significant value of ε resulted in the highest amplitude of skin friction coefficient on the velocity profile in both directions, and the Nusselt number.

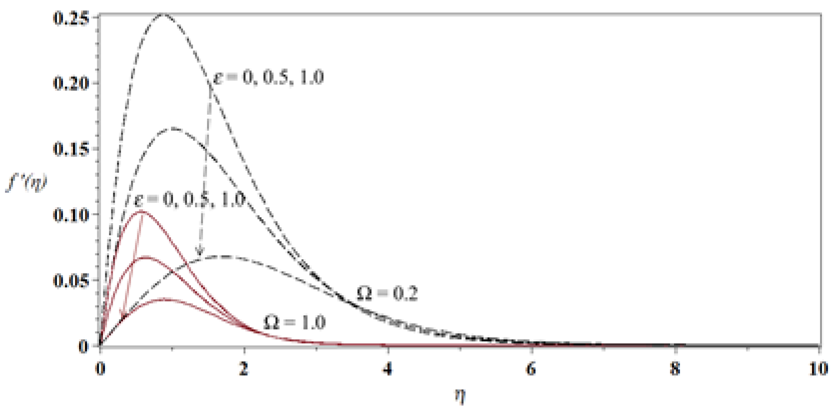

(a)

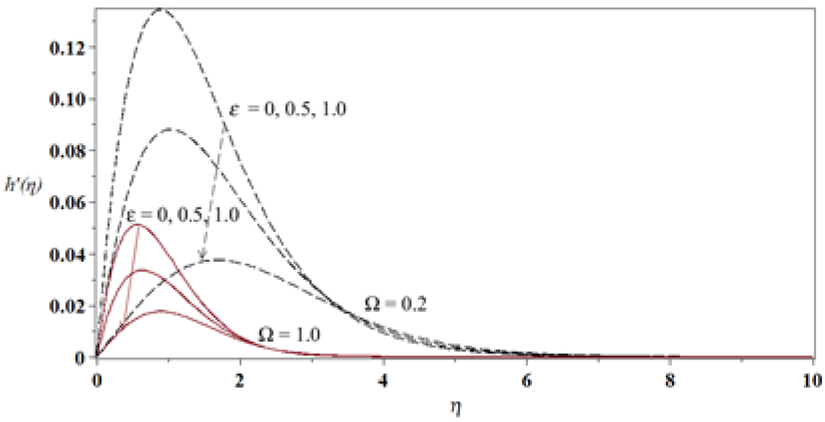

(b)

Fig. 3. The velocity profiles in (a) $x-$ and (b) $y-$direction for various values of ε and Ω

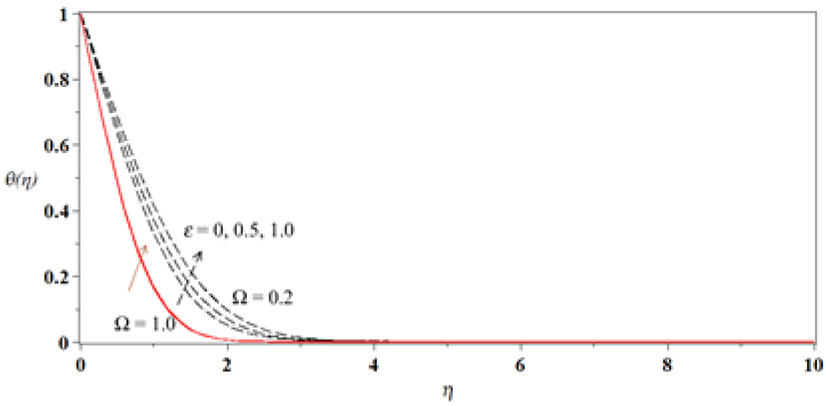

Fig. 4. The temperature profiles for various values of ε and Ω

Table 2
Physical quantities of the flow field for various values of ε with $\Omega = 0.2$

ε	$f''(\eta,0)$			$h''(\eta,0)$			$-\theta'(\eta,0)$		
τ	0	0.5	1	0	0.5	1	0	0.5	1
0.5	0.60398	0.63206	0.65690	0.30729	0.32299	0.33712	1.27601	1.30000	1.32245
1.0	0.68418	0.39151	0.06746	0.35488	0.20303	0.03718	0.51993	0.47082	0.41907
1.5	0.68692	0.67337	0.65023	0.35792	0.34824	0.33212	0.85191	0.77755	0.66589
2.0	0.68558	0.95928	1.22489	0.35752	0.50146	0.64337	0.67631	0.71917	0.75307
2.5	0.71005	0.69756	0.71005	0.35767	0.36559	0.37348	0.77851	0.83087	0.87073
3.0	0.68544	0.39164	0.06829	0.35756	0.20489	0.03924	0.71792	0.67026	0.61923

The velocity and temperature distribution are shown in Figure 5 and 6 with the increment of ϕ_{hnf} parameters. The figure shows that the increase of ϕ_{hnf} decreases the velocity profile in both of the directions but increases the temperature curve. The result of the temperature profile hs indicated that the presence of hybrid nanoparticles has enhanced the thermal conductivity of the fluid. This is because the nanoparticles have higher thermal conductivity as compared with the base fluid. The Nusselt number that is defined as the rate of heat transfer at the body surface has also shown an incline behavior for ϕ_{hnf} as seen in Table 3. Besides that, ϕ_{hnf} has also increased the skin friction coefficient in both directions as depicted in Table 3. An additional force is produced at the surface of the boundary since there is additional friction that is contributed by the nanoparticles.

A comparison study is conducted by comparing present results with a published work to measure the accuracy of the method and algorithm applied in solving the system of equations. Table 4 and 5 shows the comparison between the solutions of Hamdan *et al.,* [33] and the results obtained in the present study with various value of c. By limiting the flow case with $C_1 = C_2 = C_3 = C_4 = 1$, $\Pr = 0.72$, $\varepsilon = 0.3$, $\tau = 2$, and $\Omega = 0.2$, the comparison results of physical quantities was conducted. f'' and h'' are the skin friction coefficient subjected to $x-$ and $y-$direction while θ' is the Nusselt number. The results of the present study are in a very good agreement with the outputs provided in the literature as shown below:

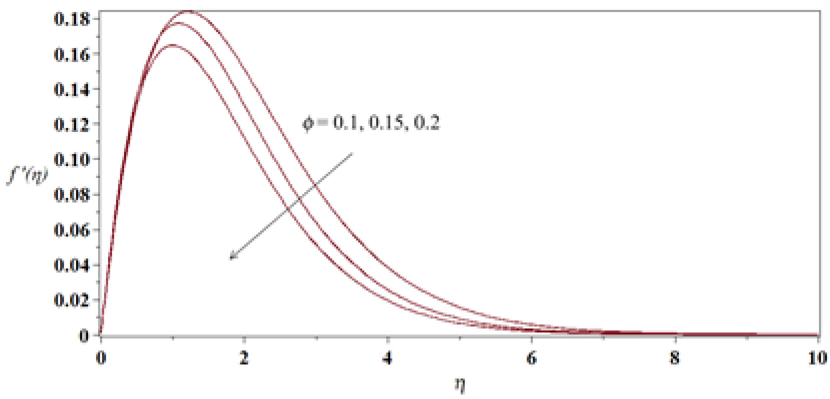

(a)

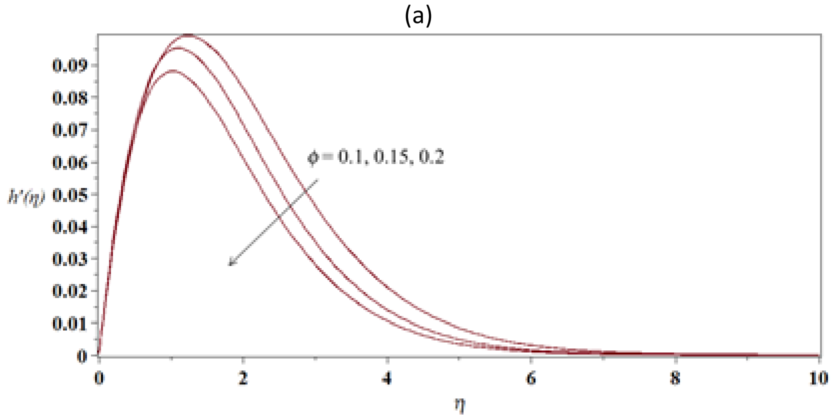

(b)

Fig. 5. The velocity profiles in (a) $x-$ and (b) $y-$direction for various values of the volume fraction ϕ of the hybrid nanoparticles

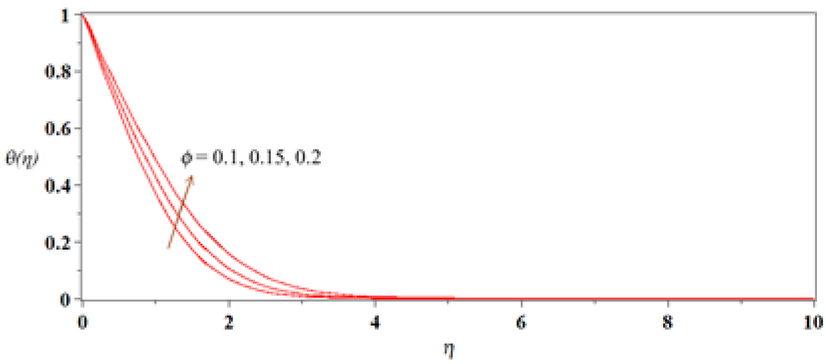

Fig. 6. The temperature profiles for various values of the volume fraction ϕ of the hybrid nanoparticles

Table 3
Physical quantities of the flow field for various values of the volume fraction ϕ

ϕ_{hnf}	C_{fx}	C_{fy}	Nu
0.10	0.683940	0.354682	0.821983
0.15	0.947592	0.493263	0.871759
0.20	1.291783	0.673720	0.910540

Table 4
Comparison of local skin frictions and Nusselt number with Hamdan *et al.,* [33] for $C_1 = C_2 = C_3 = C_4 = 1,\ \tau = 1.5$ and various values of c

c	Hamdan *et al.,* [33]		Present	
	$f'(0,\tau)$	$h'(0,\tau)$	$f'(0,\tau)$	$h'(0,\tau)$
0	0.8235	0	0.8310	0
0.5	0.7669	0.4108	0.7817	0.4153
1.0	0.7328	0.7328	0.7507	0.7507

Table 5
Comparison of local skin frictions and Nusselt number with Hamdan *et al.,* [33] for $C_1 = C_2 = C_3 = C_4 = 1$, Pr = 0.72, $\varepsilon = 0.3$, $\tau = 2$, $\Omega = 0.2$ and various value of *c*

c	η	Hamdan *et al.,* [33]			Present		
		$f'(\eta,\tau)$	$h'(\eta,\tau)$	$\theta(\eta,\tau)$	$f'(\eta,\tau)$	$h'(\eta,\tau)$	$\theta(\eta,\tau)$
	1.0	0.4450	0.2500	0.5690	0.4454	0.2493	0.5638
0.5	2.0	0.3200	0.1770	0.2450	0.3197	0.1798	0.2451
	3.0	0.1500	0.0840	0.0890	0.1491	0.0820	0.0895
	1.0	0.4030	0.4050	0.5120	0.4048	0.4047	0.5309
1.0	2.0	0.2700	0.2670	0.1900	0.2603	0.2678	0.2089
	3.0	0.1030	0.1090	0.0680	0.1067	0.1067	0.0683

4. Conclusion

The theoretical study of boundary layer hybrid nanofluid flow near a three-dimensional stagnation point was numerically investigated. The flow system consisted of Cu-Al_2O_3 water-based hybrid nanofluid with no-slip boundary conditions. The g-jitter effect was considered in the microgravity environment. The fluid system was mathematically formulated into an equation system that was subjected to the concerning impact. Based on the analysis, we can conclude that:

i. Increasing the volume fraction of hybrid nanoparticles increased the temperature profile, skin friction coefficients, and Nusselt number
ii. A 10.77% increment in heat transfer rate occurred when the hybrid nanoparticles volume fractions, ϕ_{hnf} were increased from 0.1 to 0.2.
iii. The amplitude of the gravity modulation provided a fluctuating behavior on the fluid system.
iv. The amplitude, ε of the gravity modulation increased the velocity profiles and the local skin friction. Consequently, the velocity profile in both directions decreased as the frequency of the gravity modulation, Ω increased.
v. The curvature ratio, c, of the stagnation point could determine the geometry and significantly impact the fluid characteristic.

Acknowledgment

The authors would like to acknowledge the Ministry of Higher Education Malaysia and Research Management Centre-UTM, Universiti Teknologi Malaysia (UTM) for financial support through vote numbers FRGS/1/2019/STG06/UTM/02/15.

References

[1] Choi, S. US, and Jeffrey A. Eastman. *Enhancing thermal conductivity of fluids with nanoparticles*. No. ANL/MSD/CP-84938; CONF-951135-29. Argonne National Lab.(ANL), Argonne, IL (United States), 1995.

[2] Buongiorno, Jacopo. "Convective transport in nanofluids." *J. Heat Transfer* 128, no. 3 (2006): 240-250. https://doi.org/10.1115/1.2150834

[3] Tiwari, Raj Kamal, and Manab Kumar Das. "Heat transfer augmentation in a two-sided lid-driven differentially heated square cavity utilizing nanofluids." *International Journal of heat and Mass transfer* 50, no. 9-10 (2007): 2002-2018. https://doi.org/10.1016/j.ijheatmasstransfer.2006.09.034

[4] Borrelli, Alessandra, Giulia Giantesio, Maria Cristina Patria, N. C. Roşca, A. V. Roşca, and Ioan Pop. "Buoyancy effects on the 3D MHD stagnation-point flow of a Newtonian fluid." *Communications in Nonlinear Science and Numerical Simulation* 43 (2017): 1-13. https://doi.org/10.1016/j.cnsns.2016.06.022

[5] Khan, Mair, T. Salahuddin, A. Tanveer, M. Y. Malik, and Arif Hussain. "Change in internal energy of thermal diffusion stagnation point Maxwell nanofluid flow along with solar radiation and thermal conductivity." *Chinese Journal of Chemical Engineering* 27, no. 10 (2019): 2352-2358. https://doi.org/10.1016/j.cjche.2018.12.023

[6] Bhatti, Muhammad Mubashir, S. R. Mishra, Tehseen Abbas, and Mohammad Mehdi Rashidi. "A mathematical model of MHD nanofluid flow having gyrotactic microorganisms with thermal radiation and chemical reaction effects." *Neural Computing and Applications* 30, no. 4 (2018): 1237-1249. https://doi.org/10.1007/s00521-016-2768-8

[7] Hayat, Tasawar, Arsalan Aziz, Taseer Muhammad, and Ahmed Alsaedi. "Three-dimensional flow of nanofluid with heat and mass flux boundary conditions." *Chinese journal of physics* 55, no. 4 (2017): 1495-1510. https://doi.org/10.1016/j.cjph.2017.05.005

[8] Hayat, Tasawar, Maria Imtiaz, Ahmed Alsaedi, and Marwan A. Kutbi. "MHD three-dimensional flow of nanofluid with velocity slip and nonlinear thermal radiation." *Journal of Magnetism and Magnetic Materials* 396 (2015): 31-37. https://doi.org/10.1016/j.jmmm.2015.07.091

[9] Mahanthesh, B., B. J. Gireesha, and Rama SR Gorla. "Mixed convection squeezing three-dimensional flow in a rotating channel filled with nanofluid." *International Journal of Numerical Methods for Heat & Fluid Flow* (2016). https://doi.org/10.1108/HFF-03-2015-0087

[10] Dinarvand, Saeed, Reza Hosseini, and Ioan Pop. "Axisymmetric mixed convective stagnation-point flow of a nanofluid over a vertical permeable cylinder by Tiwari-Das nanofluid model." *Powder Technology* 311 (2017): 147-156. https://doi.org/10.1016/j.powtec.2016.12.058

[11] Lin, Yanhai, Botong Li, Liancun Zheng, and Goong Chen. "Particle shape and radiation effects on Marangoni boundary layer flow and heat transfer of copper-water nanofluid driven by an exponential temperature." *Powder Technology* 301 (2016): 379-386. https://doi.org/10.1016/j.powtec.2016.06.029

[12] Kandasamy, R., Radiah Mohamad, and Muhaimin Ismoen. "Impact of chemical reaction on Cu, Al2O3 and SWCNTs–nanofluid flow under slip conditions." *Engineering Science and Technology, an International Journal* 19, no. 2 (2016): 700-709. https://doi.org/10.1016/j.jestch.2015.11.011

[13] Suresh, S., K. P. Venkitaraj, and P. Selvakumar. "Synthesis, Characterisation of Al2O3-Cu Nano composite powder and water based nanofluids." In *Advanced Materials Research*, vol. 328, pp. 1560-1567. Trans Tech Publications Ltd, 2011. https://doi.org/10.1016/j.expthermflusci.2011.11.007

[14] Hemmat, M., and A. A. Esfe. "Abbasian Arani, M. Rezaie, W.-M. Yan, A. Karimipour, Experimental determination of thermal conductivity and dynamic viscosity of Ag–MgO/water hybrid nanofluid." *Int. Commun. Heat Mass Transf.* 66 (2015): 189-195. https://doi.org/10.1016/j.icheatmasstransfer.2015.06.003

[15] Esfe, Mohammd Hemmat, Somchai Wongwises, Ali Naderi, Amin Asadi, Mohammad Reza Safaei, Hadi Rostamian, Mahidzal Dahari, and Arash Karimipour. "Thermal conductivity of Cu/TiO2–water/EG hybrid nanofluid: Experimental data and modeling using artificial neural network and correlation." *International communications in heat and mass transfer* 66 (2015): 100-104. https://doi.org/10.1016/j.icheatmasstransfer.2015.05.014

[16] Harandi, Saeed Sarbolookzadeh, Arash Karimipour, Masoud Afrand, Mohammad Akbari, and Annunziata D'Orazio. "An experimental study on thermal conductivity of F-MWCNTs–Fe3O4/EG hybrid nanofluid: effects of temperature and concentration." *International Communications in Heat and Mass Transfer* 76 (2016): 171-177. https://doi.org/10.1016/j.icheatmasstransfer.2016.05.029

[17] Moghadassi, Abdolreza, Ehsan Ghomi, and Fahime Parvizian. "A numerical study of water based Al2O3 and Al2O3–Cu hybrid nanofluid effect on forced convective heat transfer." *International Journal of Thermal Sciences* 92 (2015): 50-57. https://doi.org/10.1016/j.ijthermalsci.2015.01.025

[18] HUMINIC, Gabriela, and Angel HUMINIC. "Entropy generation of nanofluid and hybrid nanofluid flow in thermal systems." *J. Mol. Liq. doi* 10. https://doi.org/10.1016/j.molliq.2020.112533

[19] Kashyap, Dhrubajyoti, and Anoop K. Dass. "Effect of boundary conditions on heat transfer and entropy generation during two-phase mixed convection hybrid Al2O3-Cu/water nanofluid flow in a cavity." *International Journal of Mechanical Sciences* 157 (2019): 45-59. https://doi.org/10.1016/j.ijmecsci.2019.04.014

[20] Wahid, Nur Syahirah, Norihan Md Arifin, Najiyah Safwa Khashi'ie, Rusya Iryanti Yahaya, Ioan Pop, Norfifah Bachok, and Mohd Ezad Hafidz Hafidzuddin. "Three-Dimensional Radiative Flow of Hybrid Nanofluid Past a Shrinking Plate with Suction." *Journal of Advanced Research in Fluid Mechanics and Thermal Sciences* 85, no. 1 (2021): 54-70. https://doi.org/10.37934/arfmts.85.1.5470

[21] Khashi'ie, Najiyah Safwa, Iskandar Waini, Ioan Pop, Nurul Amira Zainal, and Abdul Rahman Mohd Kasim. "Axisymmetric Hybrid Nanofluid Flow Due to a Convectively Heated Stretching/Shrinking Disk." *Journal of Advanced Research in Fluid Mechanics and Thermal Sciences* 85, no. 1 (2021): 113-124. https://doi.org/10.37934/arfmts.85.1.113124

[22] Guo, Jun, Zuogang Chen, and Yuanxing Dai. "Numerical study on self-propulsion of a waterjet propelled trimaran." *Ocean Engineering* 195 (2020): 106655. https://doi.org/10.1016/j.oceaneng.2019.106655

[23] Bachok, Norfifah, Anuar Ishak, Roslinda Nazar, and Ioan Pop. "Flow and heat transfer at a general three-dimensional stagnation point in a nanofluid." *Physica B: Condensed Matter* 405, no. 24 (2010): 4914-4918. https://doi.org/10.1016/j.physb.2010.09.031

[24] Ghasemian, Amirhossein, Saeed Dinarvand, Armen Adamian, and Mikhail A. Sheremet. "Unsteady general three-dimensional stagnation point flow of a maxwell/Buongiorno non-Newtonian nanofluid." *Journal of Nanofluids* 8, no. 7 (2019): 1544-1559. https://doi.org/10.1166/jon.2019.1701

[25] Uddin, Md Jashim, W. A. Khan, A. I. Ismail, and O. Anwar Bég. "Computational study of three-dimensional stagnation point nanofluid bioconvection flow on a moving surface with anisotropic slip and thermal jump effect." *Journal of Heat Transfer* 138, no. 10 (2016). https://doi.org/10.1115/1.4033581

[26] Sulochana, C., and N. Sandeep. "Stagnation point flow and heat transfer behavior of Cu–water nanofluid towards horizontal and exponentially stretching/shrinking cylinders." *Applied Nanoscience* 6, no. 3 (2016): 451-459. https://doi.org/10.1007/s13204-015-0451-5

[27] Rehman, Fiaz Ur, S. Nadeem, and Rizwan Ul Haq. "Heat transfer analysis for three-dimensional stagnation-point flow over an exponentially stretching surface." *Chinese journal of physics* 55, no. 4 (2017): 1552-1560. https://doi.org/10.1016/j.cjph.2017.05.006

[28] Zainal, Nurul Amira, Kohilavani Naganthran, and Roslinda Nazar. "Unsteady MHD Rear Stagnation-Point Flow of a Hybrid Nanofluid with Heat Generation/Absorption Effect." *Journal of Advanced Research in Fluid Mechanics and Thermal Sciences* 87, no. 1 (2021): 41-51. https://doi.org/10.37934/arfmts.87.1.4151

[29] Nadeem, S., Nadeem Abbas, and A. U. Khan. "Characteristics of three dimensional stagnation point flow of Hybrid nanofluid past a circular cylinder." *Results in physics* 8 (2018): 829-835. https://doi.org/10.1016/j.rinp.2018.01.024

[30] Abbas, Nadeem, M. Y. Malik, M. S. Alqarni, and S. Nadeem. "Study of three dimensional stagnation point flow of hybrid nanofluid over an isotropic slip surface." *Physica A: Statistical Mechanics and its Applications* 554 (2020): 124020. https://doi.org/10.1016/j.physa.2019.124020

[31] Khashi'ie, Najiyah Safwa, Norihan Md Arifin, Ioan Pop, Roslinda Nazar, Ezad Hafidz Hafidzuddin, and Nadihah Wahi. "Non-axisymmetric Homann stagnation point flow and heat transfer past a stretching/shrinking sheet using hybrid nanofluid." *International Journal of Numerical Methods for Heat & Fluid Flow* (2020). https://doi.org/10.1108/HFF-11-2019-0824

[32] Ghadikolaei, S. S., M. Yassari, H. Sadeghi, Kh Hosseinzadeh, and D. D. Ganji. "Investigation on thermophysical properties of Tio2–Cu/H2O hybrid nanofluid transport dependent on shape factor in MHD stagnation point flow." *Powder technology* 322 (2017): 428-438. https://doi.org/10.1016/j.powtec.2017.09.006

[33] Hamdan, Fakhru Ridhwan, Mohamad Hidayad Ahmad Kamal, Noraihan Afiqah Rawi, Ahmad Qushairi Mohamad, Anati Ali, Mohd Rijal Ilias, and Sharidan Shafie. "G-jitter free convection flow near a three-dimensional stagnation-point region with internal heat generation." *Journal of Advanced Research in Fluid Mechanics and Thermal Sciences* 67, no. 1 (2020): 119-135.

[34] Uddin, Mohammed J., Waqar A. Khan, and Norsarahaida S. Amin. "g-Jitter mixed convective slip flow of nanofluid past a permeable stretching sheet embedded in a Darcian porous media with variable viscosity." *PloS one* 9, no. 6 (2014): e99384. https://doi.org/10.1371/journal.pone.0099384

[35] Bhadauria, B. S., Ajay Singh, and Vineet Kumar. "Nonlinear g-jitter thermal instability in nanofluid in the presence of throughflow and heat source." *Advanced Science, Engineering and Medicine* 10, no. 7-8 (2018): 705-711. https://doi.org/10.1166/asem.2018.2221

[36] Agarwal, Shilpi, and Puneet Rana. "Influence of g–jitter on the Rayleigh-Bénard convection in nanofluids with internal heat source." In *AIP Conference Proceedings*, vol. 1897, no. 1, p. 020013. AIP Publishing LLC, 2017. https://doi.org/10.1063/1.5008692

[37] Rawi, Noraihan Afiqah, Abdul Rahman Mohd Kasim, Zaiton Mat Isa, Aurangzaib Mangi, and Sharidan Shafie. "G-jitter effects on the mixed convection flow of nanofluid past an inclined stretching sheet." *Frontiers in Heat and Mass Transfer (FHMT)* 8 (2017). https://doi.org/10.5098/hmt.8.12

[38] Rawi, Noraihan Afiqah, Mohd Rijal Ilias, Zaiton Mat Isa, and Sharidan Shafie. "Effect of gravity modulation on mixed convection flow of second grade fluid with different shapes of nanoparticles." *Malaysian Journal of Fundamental and Applied Sciences* 13, no. 2 (2017): 132-136. https://doi.org/10.11113/mjfas.v13n2.643

[39] RAWI, N. AFIQAH, Y. JIANN LIM, A. RAHMAN M. KASIM, MUKHETA ISA, and SHARIDAN SHAFIE. "g-Jitter Induced Free Convection of Heat and Mass Transfer Flow near a Two-Dimensional Stagnation Point in Micropolar Fluid." Adv. Math. Stat. Sci., pp. 254-262, 2015.

[40] Shafie, Sharidan, Norsarahaida Amin, and Ioan Pop. "g-Jitter free convection flow in the stagnation-point region of a three-dimensional body." *Mechanics Research Communications* 34, no. 2 (2007): 115-122. https://doi.org/10.1016/j.mechrescom.2006.05.004

[41] Rees, D. A. S., and I. Pop. "g-Jitter induced free convection near a stagnation point." *Heat and mass transfer* 37, no. 4 (2001): 403-408. https://doi.org/10.1007/s002310000178

[42] Kamal, Mohamad Hidayad Ahmad, Noraihan Afiqah Rawi, Mohd Rijal Ilias, Anati Ali, and Sharidan Shafie. "Effect of thermal radiation on a three-dimensional stagnation point region in nanofluid under microgravity environment." *Universal Journal of Mechanical Engineering* 7 (2019): 272-284. https://doi.org/10.13189/ujme.2019.070504

[43] Kamal, Mohamad Hidayad Ahmad, Anati Ali, and Sharidan Shafie. "g-jitter free convection flow of nanofluid in the three-dimensional stagnation point region." *MATEMATIKA: Malaysian Journal of Industrial and Applied Mathematics* (2019): 260-270. https://doi.org/10.11113/matematika.v35.n2.1116

[44] Prandtl, L. "On the motion of a fluid with very small viscosity." In *Proceedings of 3rd International Mathematics Congress*, pp. 484-491. 1904.

[45] Waini, Iskandar, Anuar Ishak, and Ioan Pop. "Hybrid nanofluid flow induced by an exponentially shrinking sheet." *Chinese Journal of Physics* 68 (2020): 468-482. https://doi.org/10.1016/j.cjph.2019.12.015

[46] Saqib, Muhammad, Ilyas Khan, and Sharidan Shafie. "Application of fractional differential equations to heat transfer in hybrid nanofluid: modeling and solution via integral transforms." *Advances in Difference Equations* 2019, no. 1 (2019): 1-18. https://doi.org/10.1186/s13662-019-1988-5